EUROPEAN ORGANIZATION FOR NUCLEAR RESEARCH

CERN-PPE/91-26
12 February 1991

Search for a New Weakly Interacting Particle

The ALEPH Collaboration

Abstract

A search for events of the type $e^+e^- \rightarrow l^+l^-X^0$, where X^0 can be any weakly interacting particle which couples to the Z, has been performed with the ALEPH detector at LEP, by searching for acollinear lepton pairs. Such particles can be excluded up to a mass of 7.0 GeV/c^2 for a value of the ratio of branching fractions, $Br(Z \rightarrow X^0l^+l^-)/Br(Z \rightarrow l^+l^-)$, greater than 2.5×10^{-3} if the X^0 has third component of isospin, I_3, greater than $\frac{1}{2}$ and decays to a pair of virtual gauge bosons. When this analysis is combined with the previous results of the Higgs particle searches from ALEPH, this limit can be extended to an X^0 mass of 60 GeV/c^2.

(Submitted to Physics Letters B)

D. Decamp, B. Deschizeaux, C. Goy, J.-P. Lees, M.-N. Minard

Laboratoire de Physique des Particules (LAPP), IN²P³-CNRS, 74019 Annecy-le-Vieux Cedex, France

R. Alemany, J.M. Crespo, M. Delfino, E. Fernandez, V. Gaitan, Ll. Garrido, P. Mato, Ll.M. Mir, A. Pacheco

Laboratorio de Fisica de Altas Energias, Universidad Autonoma de Barcelona, 08193 Bellaterra (Barcelona), Spain[8]

M.G. Catanesi, D. Creanza, M. de Palma, A. Farilla, G. Iaselli,[1] G. Maggi, M. Maggi, S. Natali, S. Nuzzo, M. Quattromini, A. Ranieri, G. Raso, F. Romano, F. Ruggieri, G. Selvaggi, L. Silvestris, P. Tempesta, G. Zito

INFN Sezione di Bari e Dipartimento di Fisica dell' Università, 70126 Bari, Italy

Y. Gao, H. Hu,[21] D. Huang, X. Huang, J. Lin, J. Lou, C. Qiao,[21] T. Ruan,[21] Wang, Y. Xie, D. Xu, R. Xu, J. Zhang, W. Zhao

Institute of High-Energy Physics, Academia Sinica, Beijing, The People's Republic of China[9]

W.B. Atwood,[2] F. Bird, E. Blucher, G. Bonvicini, F. Bossi, D. Brown, T.H. Burnett,[3] H. Drevermann, F. Dydak, R.W. Forty, C. Grab, R. Hagelberg, S. Haywood, J. Hilgart, B. Jost, M. Kasemann, J. Knobloch, A. Lacourt, E. Lançon, I. Lehraus, T. Lohse, A. Marchioro, M. Martinez, S. Menary, A. Minten, A. Miotto, R. Miquel, H.-G. Moser, J. Nash, P. Palazzi, F. Ranjard, G. Redlinger, A. Roth, J. Rothberg,[3] H. Rotscheidt, R. St.Denis, D. Schlatter, M. Takashima, M. Talby,[4] W. Tejessy, H. Wachsmuth, S. Wasserbaech, S. Wheeler, W. Wiedenmann, W. Witzeling, J. Wotschack

European Laboratory for Particle Physics (CERN), 1211 Geneva 23, Switzerland

Z. Ajaltouni, M. Bardadin-Otwinowska, A. Falvard, R. El Fellous, P. Gay, J. Harvey, P. Henrard, J. Jousset, B. Michel, J-C. Montret, D. Pallin, P. Perret, J. Proriol, F. Prulhière, G. Stimpfl

Laboratoire de Physique Corpusculaire, Université Blaise Pascal, IN²P³-CNRS, Clermont-Ferrand, 63177 Aubière, France

J.D. Hansen, J.R. Hansen, P.H. Hansen, R. Møllerud, E.R. Nielsen, B.S. Nilsson

Niels Bohr Institute, 2100 Copenhagen, Denmark[10]

I. Efthymiopoulos, E. Simopoulou, A. Vayaki

Nuclear Research Center Demokritos (NRCD), Athens, Greece

J. Badier, A. Blondel, G. Bonneaud, J. Bourotte, F. Braems, J.C. Brient, G. Fouque, A. Gamess, R. Guirlet, S. Orteu, A. Rosowsky, A. Rougé, M. Rumpf, R. Tanaka, H. Videau

Laboratoire de Physique Nucléaire et des Hautes Energies, Ecole Polytechnique, IN²P³-CNRS, 91128 Palaiseau Cedex, France

D.J. Candlin, E. Veitch

Department of Physics, University of Edinburgh, Edinburgh EH9 3JZ, United Kingdom[11]

G. Parrini

Dipartimento di Fisica, Università di Firenze, INFN Sezione di Firenze, 50125 Firenze, Italy

M. Corden, C. Georgiopoulos, M. Ikeda, J. Lannutti, D. Levinthal,[16] M. Mermikides, L. Sawyer

Supercomputer Computations Research Institute and Dept. of Physics, Florida State University, Tallahassee, FL 32306, USA[13,14,15]

A. Antonelli, R. Baldini, G. Bencivenni, G. Bologna,[5] P. Campana, G. Capon, V. Chiarella, B. D'Ettorre-Piazzoli,[6] G. Felici, P. Laurelli, G. Mannocchi,[6] F. Massimo-Brancaccio, F. Murtas, G.P. Murtas, G. Nicoletti, L. Passalacqua, M. Pepe-Altarelli, P. Picchi,[5] P. Zografou

Laboratori Nazionali dell'INFN (LNF-INFN), 00044 Frascati, Italy

B. Altoon, O. Boyle, A.W. Halley, I. ten Have, J.L. Hearns, J.G. Lynch, W.T. Morton, C. Raine, J.M. Scarr, K. Smith, A.S. Thompson, R.M. Turnbull

Department of Physics and Astronomy, University of Glasgow, Glasgow G12 8QQ, United Kingdom[11]

B. Brandl, O. Braun, R. Geiges, C. Geweniger, P. Hanke, V. Hepp, E.E. Kluge, Y. Maumary, A. Putzer, B. Rensch, A. Stahl, K. Tittel, M. Wunsch

Institut für Hochenergiephysik, Universität Heidelberg, 6900 Heidelberg, Fed. Rep. of Germany[17]

A.T. Belk, R. Beuselinck, D.M. Binnie, W. Cameron, M. Cattaneo, P.J. Dornan,[1] S. Dugeay, A.M. Greene, J.F. Hassard, N.M. Lieske, S.J. Patton, D.G. Payne, M.J. Phillips, J.K. Sedgbeer, G. Taylor, I.R. Tomalin, A.G. Wright

Department of Physics, Imperial College, London SW7 2BZ, United Kingdom[11]

P. Girtler, D. Kuhn, G. Rudolph

Institut für Experimentalphysik, Universität Innsbruck, 6020 Innsbruck, Austria[19]

C.K. Bowdery,[1] T.J. Brodbeck, A.J. Finch, F. Foster, G. Hughes, N.R. Keemer, M. Nuttall, A. Patel, B.S. Rowlingson, T. Sloan, S.W. Snow, E.P. Whelan

Department of Physics, University of Lancaster, Lancaster LA1 4YB, United Kingdom[11]

T. Barczewski, L.A.T. Bauerdick, K. Kleinknecht, B. Renk, S. Roehn, H.-G. Sander, M. Schmelling, H. Schmidt, F. Steeg

Institut für Physik, Universität Mainz, 6500 Mainz, Fed. Rep. of Germany[17]

J-P. Albanese, J-J. Aubert, C. Benchouk, V. Bernard, A. Bonissent, D. Courvoisier, F. Etienne, S. Papalexiou, P. Payre, B. Pietrzyk, Z. Qian

Centre de Physique des Particules, Faculté des Sciences de Luminy, IN²P³-CNRS, 13288 Marseille, France

H. Becker, W. Blum, P. Cattaneo, G. Cowan, B. Dehning, H. Dietl, M. Fernandez-Bosman, T. Hansl-Kozanecka,[22] A. Jahn, W. Kozanecki,[2,23] E. Lange, J. Lauber, G. Lütjens, G. Lutz, W. Männer, Y. Pan, R. Richter, J. Schröder, A.S. Schwarz, R. Settles, U. Stierlin, J. Thomas, G. Wolf

Max-Planck-Institut für Physik und Astrophysik, Werner-Heisenberg-Institut für Physik, 8000 München, Fed. Rep. of Germany[17]

V. Bertin, J. Boucrot, O. Callot,[1] X. Chen, A. Cordier, M. Davier, G. Ganis, J.-F. Grivaz, Ph. Heusse, P. Janot, D.W. Kim,[20] F. Le Diberder, J. Lefrançois,[1] A.-M. Lutz, J.-J. Veillet, I. Videau, Z. Zhang, F. Zomer

Laboratoire de l'Accélérateur Linéaire, Université de Paris-Sud, IN²P³-CNRS, 91405 Orsay Cedex, France

S.R. Amendolia, G. Bagliesi, G. Batignani, L. Bosisio, U. Bottigli, C. Bradaschia, M. Carpinelli, M.A. Ciocci, R. Dell'Orso, I. Ferrante, F. Fidecaro, L. Foà, E. Focardi, F. Forti, A. Giassi, M.A. Giorgi, F. Ligabue, A. Lusiani, E.B. Mannelli, P.S. Marrocchesi, A. Messineo, L. Moneta, F. Palla, G. Sanguinetti, J. Steinberger, R. Tenchini, G. Tonelli, G. Triggiani, C. Vannini, A. Venturi, P.G. Verdini, J. Walsh

Dipartimento di Fisica dell'Università, INFN Sezione di Pisa, e Scuola Normale Superiore, 56010 Pisa, Italy

J.M. Carter, M.G. Green, P.V. March, T. Medcalf, I.S. Quazi, M.R. Saich, J.A. Strong, R.M. Thomas, L.R. West, T. Wildish

Department of Physics, Royal Holloway & Bedford New College, University of London, Surrey TW20 OEX, United Kingdom[11]

D.R. Botterill, R.W. Clifft, T.R. Edgecock, M. Edwards, S.M. Fisher, T.J. Jones, P.R. Norton, D.P. Salmon, J.C. Thompson

Particle Physics Dept., Rutherford Appleton Laboratory, Chilton, Didcot, OXON OX11 OQX, United Kingdom[11]

B. Bloch-Devaux, P. Colas, C. Klopfenstein, E. Locci, S. Loucatos, E. Monnier, P. Perez, J.A. Perlas, F. Perrier, J. Rander, J.-F. Renardy, A. Roussarie, J.-P. Schuller, J. Schwindling, B. Vallage

Département de Physique des Particules Elémentaires, CEN-Saclay, 91191 Gif-sur-Yvette Cedex, France[18]

J.G. Ashman, C.N. Booth, C. Buttar, R. Carney, S. Cartwright, F. Combley, M. Dinsdale, M. Dogru, F. Hatfield, J. Martin, D. Parker, P. Reeves, L.F. Thompson

Department of Physics, University of Sheffield, Sheffield S3 7RH, United Kingdom[11]

S. Brandt, H. Burkhardt, C. Grupen, H. Meinhard, L. Mirabito, E. Neugebauer, U. Schäfer, H. Seywerd

Fachbereich Physik, Universität Siegen, 5900 Siegen, Fed. Rep. of Germany[17]

G. Apollinari, G. Giannini, B. Gobbo, F. Liello, L. Rolandi, U. Stiegler

Dipartimento di Fisica, Università di Trieste e INFN Sezione di Trieste, 34127 Trieste, Italy

L. Bellantoni, J.F. Boudreau, D. Cinabro, J.S. Conway, D.F. Cowen,[24] A.J. DeWeerd, Z. Feng, D.P.S. Ferguson, Y.S. Gao, J. Grahl, J.L. Harton, J.E. Jacobsen, R.C. Jared,[7] R.P. Johnson, B.W. LeClaire, Y.B. Pan, J.R. Pater, Y. Saadi, V. Sharma, A.M. Walsh, J.A. Wear, F.V. Weber, M.H. Whitney, Sau Lan Wu, Z.L. Zhou, G. Zobernig

Department of Physics, University of Wisconsin, Madison, WI 53706, USA[12]

---

[1] Now at CERN.
[2] Permanent adddress: SLAC, Stanford, CA 94309, USA.
[3] Permanent address: University of Washington, Seattle, WA 98195, USA.
[4] Also Centre de Physique des Particules, Faculté des Sciences, Marseille, France
[5] Also Istituto di Fisica Generale, Università di Torino, Torino, Italy.
[6] Also Istituto di Cosmo-Geofisica del C.N.R., Torino, Italy.
[7] Permanent address: LBL, Berkeley, CA 94720, USA.
[8] Supported by CAICYT, Spain.
[9] Supported by the National Science Foundation of China.
[10] Supported by the Danish Natural Science Research Council.
[11] Supported by the UK Science and Engineering Research Council.
[12] Supported by the US Department of Energy, contract DE-AC02-76ER00881.
[13] Supported by the US Department of Energy, contract DE-FG05-87ER40319.
[14] Supported by the NSF, contract PHY-8451274.
[15] Supported by the US Department of Energy, contract DE-FC0S-85ER250000.
[16] Supported by SLOAN fellowship, contract BR 2703.
[17] Supported by the Bundesministerium für Forschung und Technologie, Fed. Rep. of Germany.
[18] Supported by the Institut de Recherche Fondamentale du C.E.A..
[19] Supported by Fonds zur Förderung der wissenschaftlichen Forschung, Austria.
[20] Supported by the Korean Science and Engineering Foundation and Ministry of Education.
[21] Supported by the World Laboratory.
[22] On leave of absence from MIT, Cambridge, MA 02139, USA.
[23] Supported by Alexander von Humboldt Fellowship, Germany.
[24] Now at California Institute of Technology, Pasadena, California, USA.

1 Introduction

Recent searches performed with ALEPH at LEP have excluded the existence of a Minimal Standard Model (MSM) Higgs boson [1] up to 48.0 GeV/c^2 [2]. This paper presents a more general search for a new particle which couples to the Z and whose production and decay coupling strengths are unknown.

Events considered in this analysis are from data corresponding to a total luminosity of 7.9 pb^{-1} collected from a scan of the Z peak. The analysis procedure assumes that the X^0 escapes the detector before decaying and is *maximally stable*, that is, it decays by the same mechanism as it is produced, coupling to two virtual Z bosons (see Figure 1). For example, if X^0 has third component of weak isospin, I_3 greater than $\frac{1}{2}$, then such a decay is required. Within the framework of the Standard Model, the X^0 can also decay to two W bosons which would reduce further the X^0 lifetime. However, it will be shown in section 3 that allowing the X^0 to decay this way does not affect the result. The decay width for $X^0 \rightarrow Z^*Z^*$ is given by Kleiss [3]

$$\Gamma_{X^0} = \frac{1}{9216\pi^5}\frac{61}{504}\frac{M_{X^0}^7 g^2}{M_Z^8}\sum_{f_1,f_2} C_{f_1}C_{f_2}(v_{f_1}^2 + a_{f_1}^2)(v_{f_2}^2 + a_{f_2}^2) \quad (1)$$

where

$$g = decay\ constant \times M_Z \quad (2)$$

and $v_{f_{1,2}}$ and $a_{f_{1,2}}$ are the vector and axial vector couplings respectively of the virtual Z bosons to the fermions, $f_{1,2}$, and $C_{f_{1,2}} = 3$ for quarks and $= 1$ otherwise. The value of the ZZ^*X coupling which is excluded is then a function of luminosity, efficiency and Z^* decay channel used.

2 The ALEPH Detector

The ALEPH detector is described in detail elsewhere [4]. The parts of the detector relevant to this analysis are the inner tracking chamber (ITC), the large time-projection chamber (TPC), the electromagnetic calorimeter (ECAL) and the hadron calorimeter (HCAL). A 1.5 T axial magnetic field is provided by the superconducting coil surrounding the ITC, TPC and ECAL.

The ECAL is a lead proportional tube sandwich with a total thickness corresponding to 22 radiation lengths with 45 read out layers. It is separated into three *stacks* corresponding to 4, 9 and 9 radiation lengths respectively. Anode wire signals are summed plane by plane for each module. Cathode pads of approximately 3 x 3 cm^2 from consecutive planes are connected together to form *towers* pointing to the interaction region. The HCAL is an iron streamer tube sandwich with 23 layers, segmented into 4800 projective towers. In both ECAL and HCAL, *objects* are defined as groups of hit cells topologically connected. The trigger conditions are the same as described in [5].

3 Procedure

This analysis assumes the reaction $e^+e^- \rightarrow Z^*X^0$, where $Z^* \rightarrow l^+l^-$, and the X^0 escapes the detector before decaying; l refers throughout this text to either electrons or muons. Events of this type will contain a pair of acollinear leptons and no energy (unassociated with the charged tracks) deposited in the calorimeters. In order to cover the largest mass range possible for X^0 it is necessary to define two sets of cuts which are determined from investigation of Monte Carlo events for the process $e^+e^- \rightarrow l^+l^-X^0$ at various values of M_{X^0}. Such events are generated with

X^0 as a neutral, stable, scalar particle, and include both initial and final state radiation [6]. The simulated events are processed by the same reconstruction and analysis programs as used for data.

For *low* M_{X^0}, the leptons are moderately acollinear and very energetic, whereas for *higher* M_{X^0}, the events are characterized by larger acollinearity and lower track energies. The crossover point between *high* and *low* mass regions has been determined by a study of the simulated events. For the lower mass range the background comes mainly from $e^+e^- \rightarrow \tau^+\tau^-$ events while in the higher mass range, the main background is from two photon scattering processes where the initial e^+e^- escape down the beam pipe. It is necessary for both selections to ensure that no photons accompany the two leptons and this is done by vetoing events with energy clusters in the calorimeters.

3.1 Event selection

Events with two and only two oppositely charged tracks are selected. The tracks are then required to have at least 4 ITC and 4 TPC coordinates. They must come within 0.2 *cm* of the beam in the plane transverse to the beam and within 5 *cm* of the interaction point in the beam direction. Furthermore, all tracks must have $\mid cos\Theta \mid < 0.95$, where Θ is the polar angle between the track and the beam axis, and have a χ^2 per degree of freedom for the fit of less than 5. The acollinearity, defined as $\pi - \eta$ where η is the angle between the tracks, must be greater than 20 *mr*. The acollinearity of these remaining events can only result from radiated photons or unobservable particle(s). The background processes at this point are:

A. $e^+e^- \rightarrow e^+e^-(\geq 1\gamma)$

B. $e^+e^- \rightarrow \mu^+\mu^-(\geq 1\gamma)$

C. $e^+e^- \rightarrow \tau^+\tau^-(\geq 0\gamma)$

D. $e^+e^- \rightarrow (e^+e^-)e^+e^-$

E. $e^+e^- \rightarrow (e^+e^-)\mu^+\mu^-$

F. $e^+e^- \rightarrow (e^+e^-)\tau^+\tau^-$

We define an event plane, from the momentum vectors of the tracks, with the normal vector

$$\hat{n} \equiv \frac{\vec{P_{l+}} \times \vec{P_{l-}}}{\mid \vec{P_{l+}} \times \vec{P_{l-}} \mid}. \tag{3}$$

In the case of a three body final state, all three momentum vectors lie in this event plane. In particular, for background processes A and B, if the radiated photon is an initial state photon, then the event plane will contain the beam axis. Due to the hole in the acceptance around the beam axis, such events are excluded by requiring $\zeta = \vec{z} \cdot \hat{n}$, the cosine of the angle between the beam axis and $\hat{n}$, to be greater than 0.2.

The remainder of background processes A and B contain one or more photons, and therefore a photon veto is required to exclude these events. The ECAL is read out by two independent sets of electronics: one connected to the cathode pads and the other to the anode wires for each sampling plane. For this analysis, ECAL clusters were divided into two categories. The first category (type I objects) were photons that were identified using only the ECAL pad information with the following criteria:

1. energy deposited must be greater than $700MeV$
2. No electronics noise : the cluster does not overlap identified bad electronics channels;

3a. Object points to the origin: the transverse shower centroids (barycentre) in the two stacks with the most energy point toward the origin within $300mr$;

4a. Depth profile of object: objects deposit energy among the ECAL stacks in a manner consistent with being photons;

The second category (type II objects) were photons that were identified by somewhat orthogonal considerations in the ECAL based on the wire information. In addition to criteria 1 and 2 above, the following requirements were deemed necessary:

3b. Ratio of pad and wire energies for modules containing objects must lie between 0.5 and 1.5;

4b. Timing information from wires must fall within $\pm 250ns$ of the beam crossing.

From a study of random trigger events, taken under the same running conditions as the data, the fraction of these random events which have noise which fakes either type I or type II ECAL objects is 3.5%. This has defined the veto inefficiency. The choices of a type I or type II object were made in order to maximize the efficiency for detecting photons (96% within the acceptance of the ECAL) while minimizing the veto inefficiency. To veto events which contained a photon which travelled between two ECAL modules, the HCAL was searched in the event plane region behind ± 4 *cm* of the ECAL cracks for any identified object. The region in the HCAL is limited to minimize its veto inefficiency which is found to be 2.5% for this cut.

In order to simulate the background processes, Monte Carlo events of processes A to F were generated for 2.6 times the data and normalized to the luminosity. A study of these simulated events led to the definition of two further sets of cuts, depending on the mass of X^0. For low M_{X^0} (selection 1), the $e^+e^- \rightarrow l^+l^-X^0$ events are characterized by a moderate acollinearity and high track energies, a similar topology to events in the tail of the $e^+e^- \rightarrow \tau^+\tau^- \rightarrow l^+l^- + (4\nu)$ event distributions. Figure 2 shows the distribution of $\frac{p_{track}}{E_{beam}}$ for the Monte Carlo simulation of the background processes A to F after the above cuts are made, where p_{track} is the momentum of the lowest momentum track. The data is overlayed and there is reasonable agreement. In addition, the predicted distribution for events with $M_{X^0} = 200$ MeV/c^2 is shown. A cut is made requiring $\frac{p_{track}}{E_{beam}} > 0.67$ because the signal (X^0 events) is peaked near 1 in this variable while the background events are not. The acollinearity cut has been purposely left loose up to this point to allow a higher statistics check against the Monte Carlo background processes (see Table 1). To optimize the sensitivity of the selection, the acollinearity cut is raised to 50 *mr* for the low mass X^0 search.

For a high M_{X^0} (selection 2), the cut on $\frac{p_{track}}{E_{beam}}$ is replaced by a cut on the sum of the momenta of the observed tracks: $P_{chgd} = \mid \vec{P}_{l+} \mid + \mid \vec{P}_{l-} \mid > 20GeV$. This cut reduces background types D to F. The acollinearity cut is further increased to 150 *mr* to reduce background type C. Figure 3 shows the P_{chgd} distribution for Monte Carlo processes D and E overlayed with the distribution expected for the process $e^+e^- \rightarrow l^+l^-X^0$ with $M_{X^0} = 5.0$GeV/c^2.

Figure 4 shows the efficiency for the two different selection procedures as a function of M_{X^0} for a completely stable X^0, ignoring the effect of a finite lifetime for the X^0. The crossover between selection 1 and selection 2 occurs at $M_{X^0} = 3.0$ GeV/c^2. Because the lifetime, τ_{X^0}, is affected by M_{X^0} and the value of the decay constant, once the X^0 has an appreciable probability to decay inside the detector the efficiency for detecting it with this method decreases like

$$N_{observed} = N_0 \, e^{-\frac{x}{\bar{x}}} \tag{4}$$

where

$$\bar{x} = \frac{c\tau_{X^0}}{M_{X^0}} \bar{p}. \tag{5}$$

In the above equations, x is the distance travelled by X^0 before decaying and $\bar{p}$ is the average momentum of an X^0 whose mass is M_{X^0}.

3.2 Results

The breakdown of events for the data and Monte Carlo is shown in Table 1 for selection 1 and in Table 2 for selection 2. The number of events remaining after cuts agrees well for the data and Monte Carlo, and is consistent with no signal. 5 events are observed where 3.5 are expected from background processes for $M_{X^0} < 3.0$ GeV/c^2, using selection 1. This yields, at 95% C.L., 10.8 events expected including background. For $M_{X^0} > 3.0$ GeV/c^2, using selection 2, also 5 events are seen where 4.4 are expected, yielding, at 95% C.L., 11.1 events expected including background. An experimental quantity, related to the production coupling ZZ*X, is defined as $RBr = Br(Z \rightarrow X^0 l^+ l^-)/Br(Z \rightarrow l^+ l^-)$ and a 95% C.L. contour can be plotted in the $RBr - M_{X^0}$ plane, which takes into account the reduction in detection efficiency as a function of lifetime, τ_{X^0}, adjusted for that particular value of coupling and mass.

Figure 5 shows the limit contour for a maximally stable X^0. The area above the line is excluded. It can be seen from this plot that such a particle is excluded up to 7.0 GeV/c^2 for a value of $RBr \geq 2.5 \times 10^{-3}$. In this case, the contour approaches an asymptotic value, corresponding to the production coupling which is excluded when the two virtual Zs each decay to two neutrinos, and are unobserved in the detector. The sharp rise at 7.0 GeV/c^2 is due to two effects: as the mass increases, the lifetime decreases, but then the value of the coupling which can be excluded increases. These two factors multiply to create a very fast variation of the limit contour (see equation 1).

The results of reference [2], which quotes an efficiency for the detection of $H^0 \rightarrow jets$, $Z^* \rightarrow \nu\bar{\nu}$ up to 60 GeV, can be reinterpreted as an excluded region in the $RBr - M_{X^0}$ plane. In order to do this, it is assumed that the X^0 decays to hadrons as would a Higgs particle. The number of events excluded at 95% C.L. is divided by the estimated number of events searched and the efficiency of detection:

$$\frac{Br(Z \rightarrow \nu\bar{\nu}X^0)}{Br(Z \rightarrow \nu\bar{\nu})} \equiv \frac{Br(Z \rightarrow l^+l^-X^0)}{Br(Z \rightarrow l^+l^-)} \equiv \frac{\#events\ excluded\ at\ 95\%\ C.L.}{(\#events\ in\ sample)(efficiency)} \qquad (6)$$

Figure 6 shows the limit contours for a maximally stable X^0. Contour A corresponds to the case where X^0 decays inside the detector, while contour B is for the case where it escapes the detector without being detected. The cross over point of the two analyses clearly depends on the lifetime of the X^0, because as the lifetime decreases and more events decay inside the detector they are thus excluded from this analysis, but are detected by the analysis which searches for decay products in the detector. To illustrate this point, Figure 7 shows the limit contours when the X^0 is allowed in addition to decay to two W bosons. The cross over point between the two analyses is now shifted to 3 GeV/c^2 in M_{X^0} but the resulting limit is unchanged. It should be noted that the region excluded has always $RBr \geq 2.5 \times 10^{-3}$, and in the high mass region an even lower value of RBr is excluded.

4 Conclusion

It can be seen from Figure 6 that any new particle, whose sole decay mode is to two virtual gauge bosons, and whose coupling to the Z is such that $RBr \geq 2.5 \times 10^{-3}$ has been excluded up to a mass of 60 GeV/c^2. It should be noted that although this analysis was performed for a scalar X^0, it is also valid if X^0 is not a scalar, provided that its decay characteristics do not preclude its observation in the above analysis.

Acknowledgements

We wish to congratulate and thank our colleagues in the LEP division for operating the LEP storage ring with continuously improving performance. We thank also the engineers and technicians in all our institutions for their support in constructing ALEPH. Those of us from non-member countries thank CERN for its hospitality.

References

[1] P.W.Higgs, Phys. Lett. 12 (1964) 132
P.W.Higgs, Phys. Lett. 13 (1964) 508
P.W.Higgs, Phys. Rev. 145 (1966) 1156
F.Englert and R.Brout, Phys. Rev. Lett. 13 (1964) 321
G.S. Guralnik, C.R.Hagan and T.W.B.Kibble, Phys. Rev. Lett. 13 (1964) 585

[2] D.Decamp et al., Phys. Lett. B 245 (1990) 298
D.Decamp et al., CERN PPE/91-19, 1990, and references therein.

[3] R.Kleiss, private communication.

[4] D.Decamp et al.,Nucl. Inst. and Methods, A294 (1990) 121-178

[5] D.Decamp et al., Phys. Lett. B 236 (1990) 233

[6] J.Hilgart, Ph.D Thesis, University of Wisconsin, Madison(1990).

Tables

		Monte Carlo Processes : # of events						
cut	*data*	*lepton pairs*			*Two photon process*			
		e^+e^-	$\mu^+\mu^-$	$\tau^+\tau^-$	e^+e^-	$\mu^+\mu^-$	$\tau^+\tau^-$	$\sum_{M.C.}$
2 good tracks	23212	12938.1	7406.9	3406.9	409.6	479.2	19.2	24659.9
acollinearity $> 20mr$	6523	3061.1	916.9	3052.7	403.8	474.2	18.8	7927.5
No ECAL object	3222	1766.9	319.6	1311.1	296.1	389.6	10.0	4093.3
Veto inefficiency	3222	1705.1	308.4	1265.2	285.7	376.0	9.6	3950.0
$\zeta > 0.2$	1221	80.9	17.5	1055.9	23.3	33.0	1.1	1210.6
No HCAL object	1093	70.9	14.5	971.7	23.0	33.0	1.1	1114.2
$\frac{P_{track}}{E_{beam}} > 0.67$	30	9.3	6.3	13.7	0.0	0.0	0.4	29.7
acollinearity $> 50mr$	5	2.3	0.8	0.4	0.0	0.0	0.0	3.5

Table 1:

		Monte Carlo Processes : # of events						
cut	*data*	*lepton pairs*			*Two photon process*			
		e^+e^-	$\mu^+\mu^-$	$\tau^+\tau^-$	e^+e^-	$\mu^+\mu^-$	$\tau^+\tau^-$	$\sum_{M.C.}$
No HCAL object	1093	70.9	14.5	971.7	23.0	33.0	1.1	1114.2
$P_{chgd} > 20.0GeV$	870	70.1	14.5	828.0	0.0	0.0	0.0	912.6
acollinearity $> 150mr$	5	0.7	0.0	3.7	0.0	0.0	0.0	4.4

Table 2:

Figure Captions

Figure 1: Feynman diagram for process $e^+e^- \rightarrow l^+l^-X^0$

Figure 2: $\frac{p_{track}}{E_{beam}}$ for background processes A - F (histogram) and data (points), overlayed with the distribution for unscaled number of $e^+e^- \rightarrow l^+l^-X^0$ events, with $M_{X^0} = 200$ MeV/c^2 (hatched).

Figure 3: P_{chgd} for 2 photon Monte Carlo events and for an unscaled number of events of the type $e^+e^- \rightarrow l^+l^-X^0$ (hatched), with $M_{X^0} = 5$ GeV/c^2.

Figure 4: Efficiency (%) versus X^0 mass for selection 1 and selection 2.

Figure 5: Limit contour produced for maximally stable X^0

Figure 6: Limit contours for a maximally stable X^0 from [2], A, and from this analysis, B.

Figure 7: Limit contours for X^0 decaying to Z^*Z^* *and* W^*W^* from [2], A, and from this analysis, B.

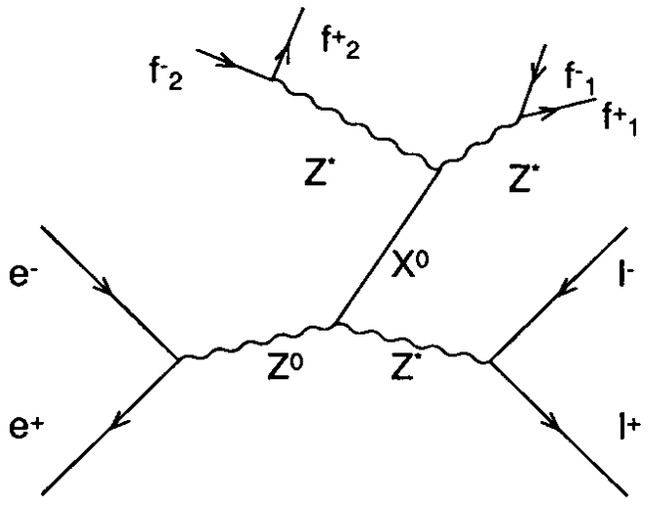

Figure 1:

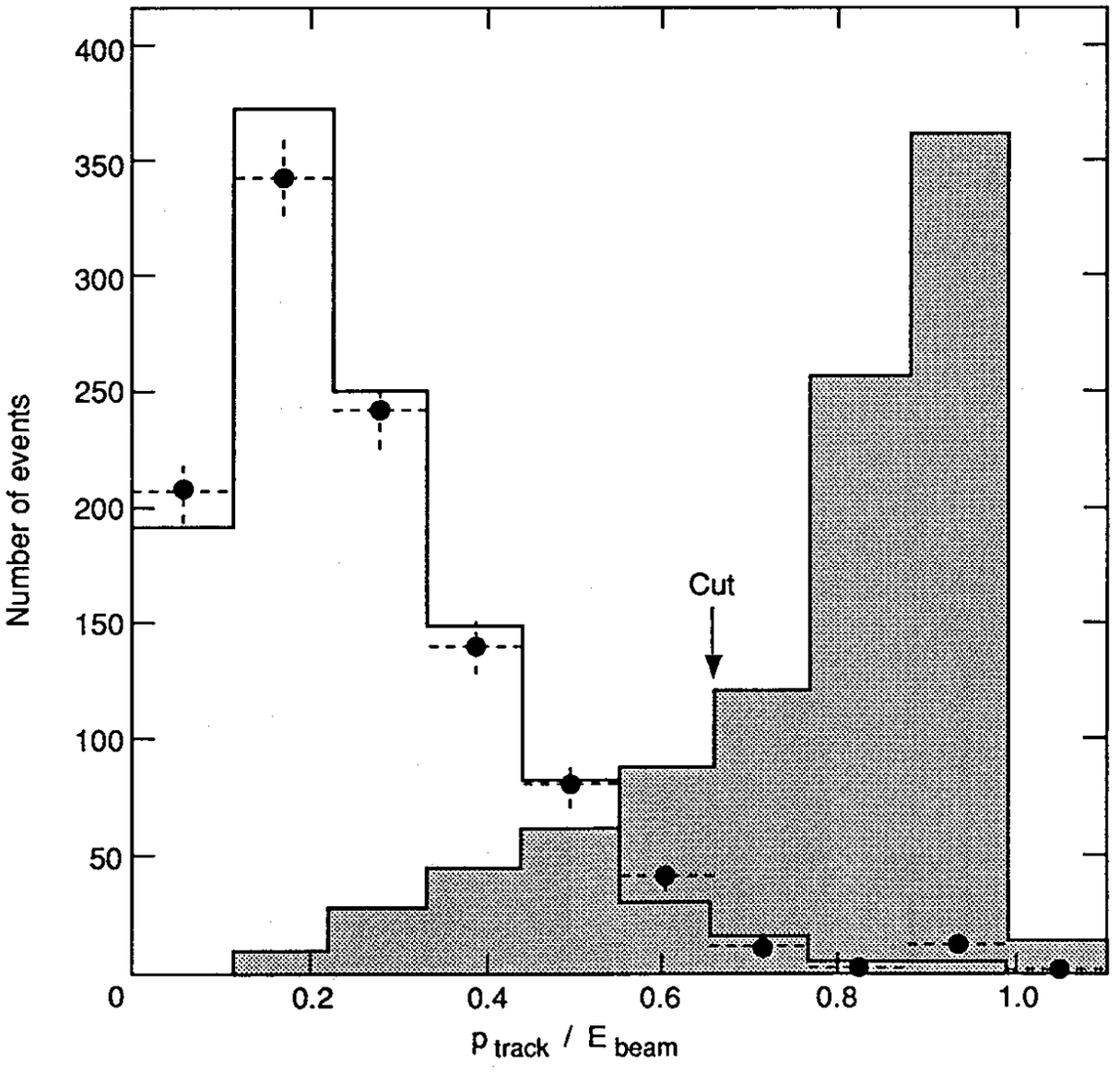
Number of events
400
350
300
250
200
150
100
50
0
0.2
0.4
0.6
0.8
1.0
Cut
p track / E beam

Figure 2:

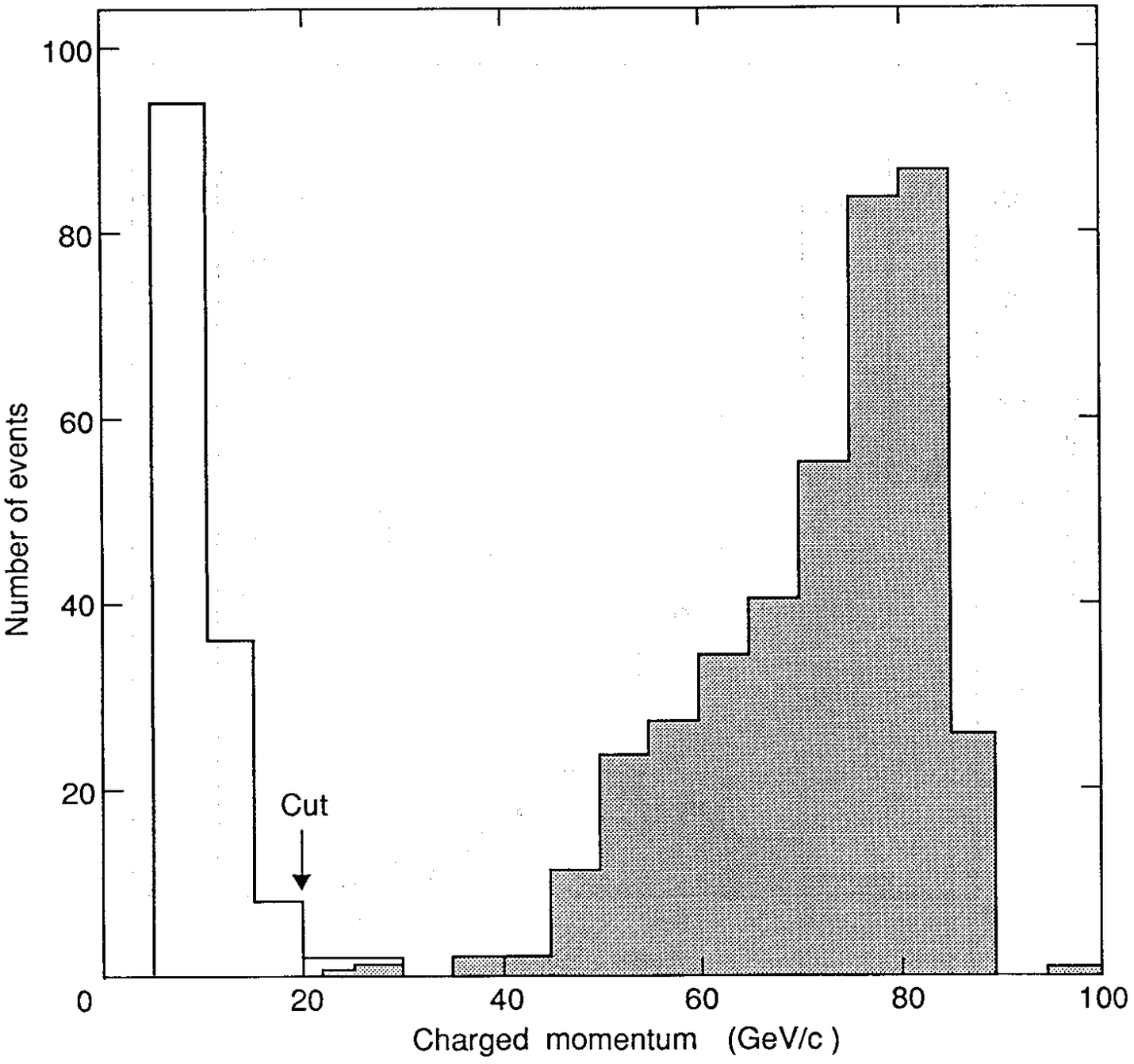
100
80
60
40
20
0
20
40
60
80
100
Number of events
Cut
Charged momentum (GeV/c)

Figure 3:

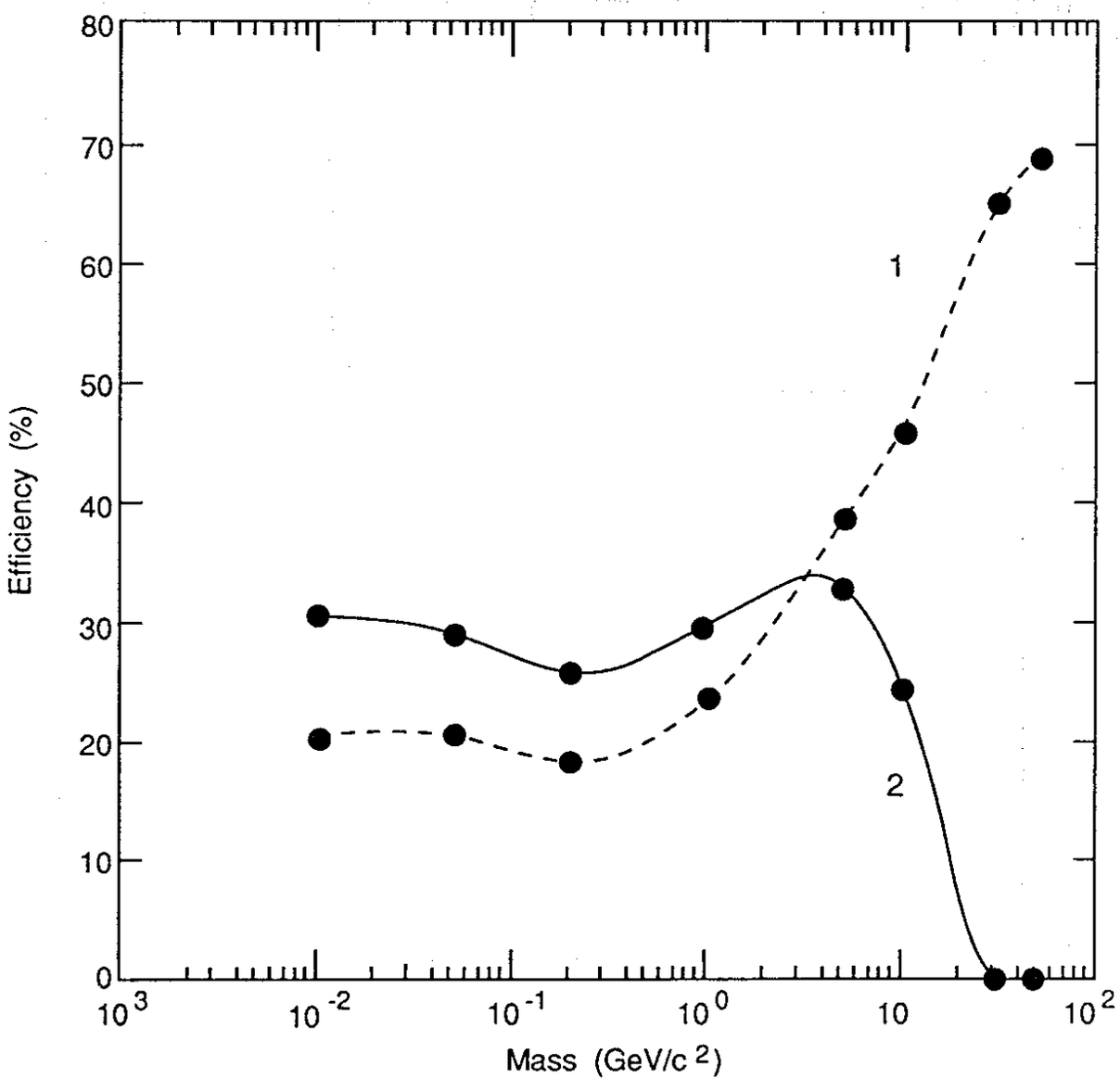
80
70
60
50
40
30
20
10
0
Efficiency (%)
1
2
10^{3}
10^{-2}
10^{-1}
10^{0}
10
10^{2}
Mass (GeV/c ^{2})

Figure 4:

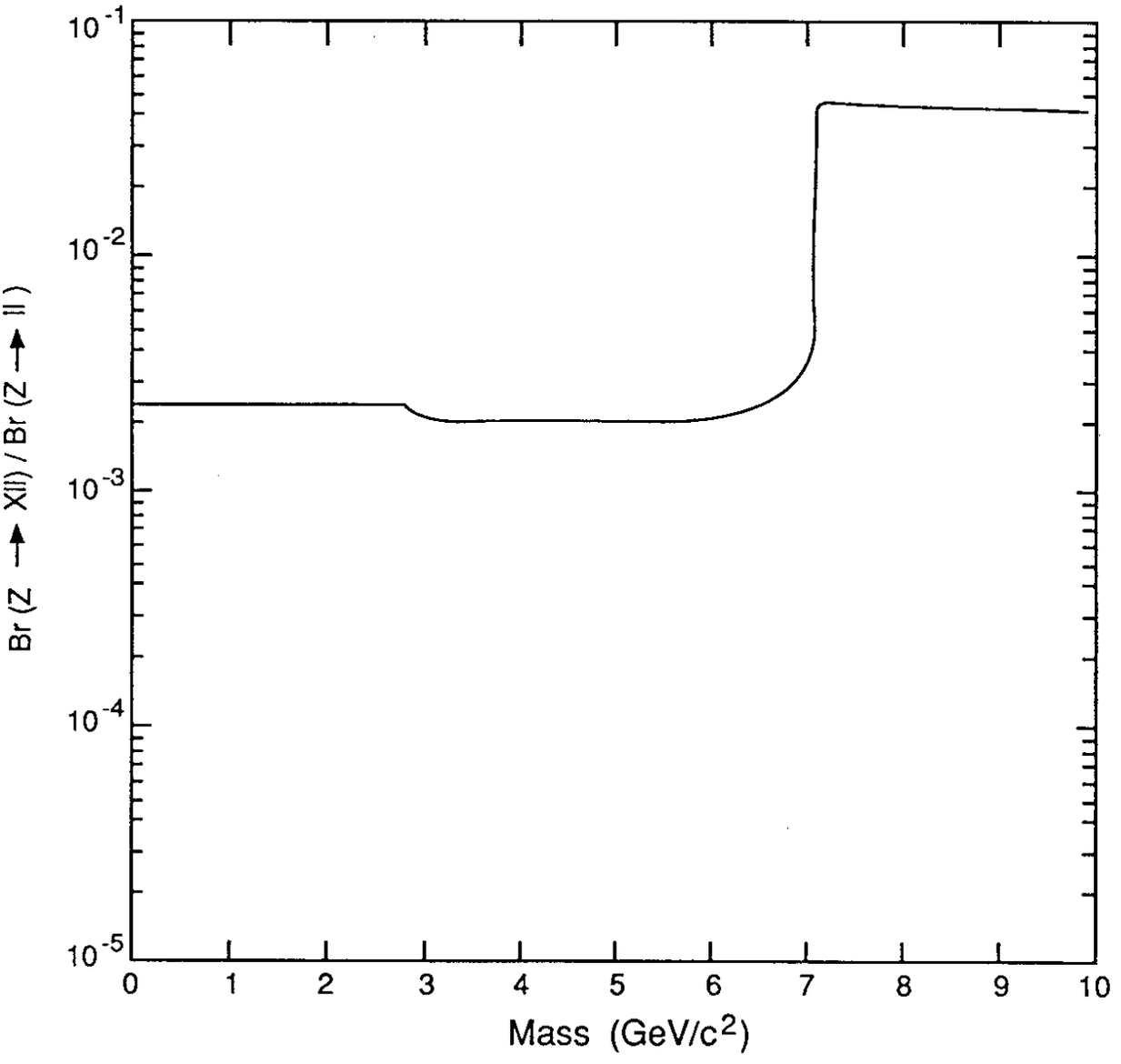

Figure 5:

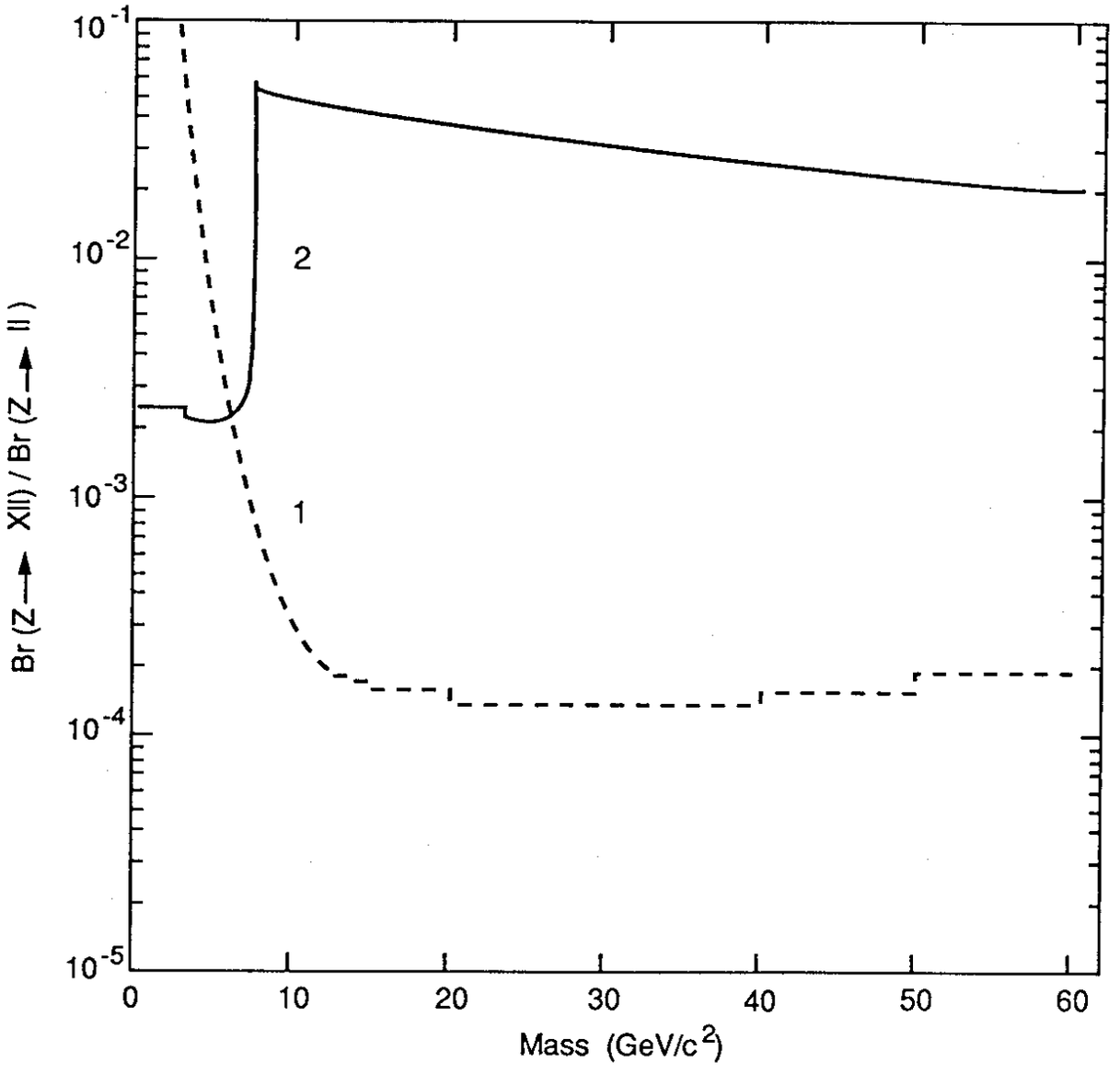
10^{-1}
10^{-2}
10^{-3}
10^{-4}
10^{-5}
Br (Z⟶ Xll) / Br (Z⟶ ll)
2
1
0
10
20
30
40
50
60
Mass (GeV/c^2)

Figure 6:

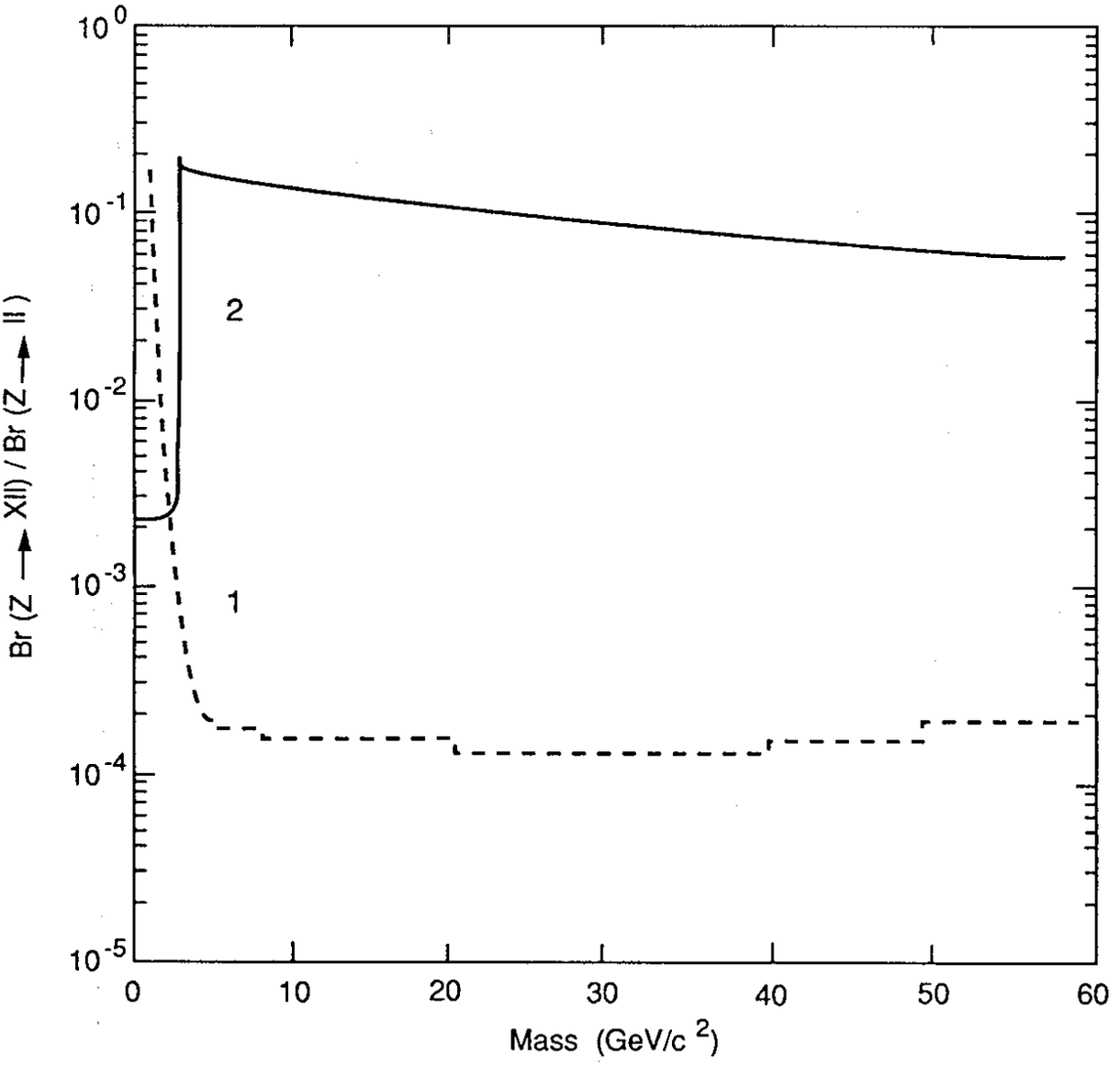

Figure 7:

Imprimé au CERN. Prix : 0.60 Fr.